Original Article

Amalgam of Ternary Solid Dispersion and P-gp Efflux Inhibition in Development of Colon-targeted Tablets of Rifaximin

Manisha S. Lalan, Pranav J. Shah[1], Ruchita Kadam, Himan P. Patel

Babaria Institute of Pharmacy, BITS Edu Campus, NH#8, P.O. Varnama, Vadodara, 391247 Gujarat, [1]Maliba Pharmacy College, Uka Tarsadia University, Maliba Campus, Gopal Vidyanagar, Bardoli-Mahuva Road, At & Po: Tarsadi 394350, Surat, Gujarat, India

Abstract

Background: Rifaximin, a BCS class IV drug, possesses low bioavailability due to low solubility and low permeability attributable to P-gp efflux. The studies attempted to develop pH-sensitive rifaximin tablets based on ternary solid dispersion (TSD) for spatial and temporal drug release in colon. **Materials and Methods:** Rifaximin TSD was prepared using Neusilin US2 as a mesoporous carrier and Poloxamer 188 as a hydrophilic carrier and P-gp inhibitor by solvent evaporation technique employing acetone at 1:5 ratio. The TSD was assessed for P-gp inhibition using the gut sac method and Caco-2 permeability studies. The TSD was compressed into tablets and coated with pH-sensitive polymers. Coating optimization was carried out using a 3^2 factorial design, wherein % coating and ratio of Eudragit S100:Eudragit L100 were the independent variables and % drug release at 2 h and % drug release at 8 h were the dependent variables. **Results:** Differential scanning calorimetry, X-ray diffraction, and scanning electron microscopy studies of rifaximin TSD suggested amorphization of the drug. Gut sac studies indicated higher mucosal to serosal permeability of rifaximin from TSD. Caco-2 permeability studies demonstrated a 4.83-fold higher permeability of rifaximin from TSD (polaxamer 25% w/w and Neusilin 55% w/w of TSD) and a significant change in efflux ratio. *In-vitro* release studies of the coated tablets displayed controlled and site-specific release at pH of the colon. **Conclusion:** Effective, stable, pH-dependent rifaximin colon-targeted tablets with enhanced dissolution, permeability, and reduced P-gp efflux were developed. The achieved merits could translate into augmented bioavailability and dose reduction. Further *in-vivo* studies on this novel formulation, which is cost-effective and industrially scalable, can improve the pharmacoeconomics of inflammatory bowel disease management.

Keywords: *Colon targeting, IBD, P-gp inhibition, rifaximin, solid dispersion adsorbate*

Introduction

The digestive tract is prone to chronic inflammation in inflammatory bowel disease (IBD).[1] The term IBD encompasses two conditions, viz., ulcerative colitis and Crohn's disease, both of which affect the colonic region and have different phenotypic representations.[2] IBD significantly impacts the quality of life of the patient with symptomatic appearances like diarrhea, fatigue, weight loss, bacterial infection, abdominal pain, and bloody stools.[3] Bacterial infections are known to complicate and aggravate the existing inflammation by disturbing the mucosal immune system through the release of proteins and superantigens. They tilt the immunological balance toward the proinflammatory side.[4] The therapeutic management paradigm in IBD is inclusive of aminosalicylates, corticosteroids, immunomodulators, biologics, and antibiotics.[5] Antibiotics have proven to be beneficial to patients with IBD because they alleviate signs of the acute stage of the ailment, e.g., diarrhea, abdominal pain, and meteorism, as well as prevent and treat septic complications, e.g., abscesses, fistulas, and toxic state by inhibiting the growth of luminal bacteria.[6]

Rifaximin is a semi-synthetic antibiotic that is rifamycin analog.[7] It exhibits broad-spectrum antibacterial activity by inhibiting bacterial DNA-dependent RNA polymerase's beta-subunit.[8] Also, it is a pregnane X receptor activator; activation of which induces inhibition of production of proinflammatory mediators.[9] Therefore, it acts dually as an anti-bacterial as well as an anti-inflammatory agent to provide relief in IBD.[10] Belonging to BCS class IV, it has low solubility and low permeability. Further, it is a P-gp substrate which

How to cite this article: Lalan MS, Shah PJ, Kadam R, Patel HP. Amalgam of ternary solid dispersion and P-gp efflux inhibition in development of colon-targeted tablets of rifaximin. J Rep Pharma Sci 2022;11:222-35.

Received: 08 Feb 2022
Accepted: 24 Aug 2022
Published: 23 Jun 2022

Address for correspondence:
Dr. Manisha S. Lalan, Babaria Institute of Pharmacy, BITS Edu Campus, NH#8, P.O. Varnama, Vadodara, 391247 Gujarat, India.
E-mail: manisha_lalan79@yahoo.co.in

Access this article online

Website: www.jrpsjournal.com

DOI: 10.4103/jrptps.JRPTPS_21_22

Quick Response Code:

translates to significant drug efflux in luminal contents.[11] By administering rifaximin in conventional dosage forms such as tablets or capsules, the drug releases into the stomach and spreads throughout the stomach and intestine.[12] The low solubility, P-gp efflux, and absence of site-specific localization of the drug are responsible for low bioavailability (< 0.4%), and increased frequency of drug administration is mandated to reach an effective concentration in the colonic region.[9]

Literature review reveals several studies on rifaximin focussed on solubility enhancement and colon targeting. Cyclodextrin complexes, amorphous solid dispersions, and nanosuspensions have been explored for solubility enhancement.[13-15] Colon-targeted tablets and multi-particulate systems have been prepared for site-specific delivery.[16,17] Nanocarrier-based colon-targeted delivery of rifaximin has also been attempted.[18,19] However, the approaches explored either have focussed on solubility enhancement as the primary means of improving bioavailability or they are costly and instrument-intensive approaches with difficulty in scaling up. Thus, there is an unmet need to prepare an easily scalable formulation that can simultaneously increase the dissolution and permeability by inhibiting P-gp efflux. This will boost the bioavailability of the drug and open up the possibility of dose reduction and cost diminution, dose-related side effects. Further, the colon-targeted formulation is required, so that the drug is specifically released in the colonic region and off-target toxicities are minimized.[20]

Among different approaches to improve the dissolution of the drug, one industrially scalable approach is the preparation of solid dispersions.[21] However, solid dispersions pose constraints in pulverization and compression and have flowability issues. Further, the drug is present in a higher-energy metastable amorphous form in solid dispersion, which has a tendency to revert to the crystalline form on storage. The adsorption of solid dispersion on porous carriers generates ternary systems which can display the benefits of solid dispersions as well as leverage the benefits of the mesoporous carriers.[22] Neusilin US2 is a mesoporous carrier with a large surface area (300 m^2/g) and small particle size (60–120 µm). The ternary solid dispersion (TSD) of drug, polymer, and porous carrier can be easily compressed into tablets as Neusilin imparts excellent flowability to the blend. Many pharmaceutical excipients such as poloxamers and polysorbates can inhibit the P-gp efflux system by inhibiting the ATPase activity of P-gp, which could lead to depletion of sufficient energy of P-gp efflux mechanism.[23] As a non-ionic surfactant, poloxamers have been widely used for wetting and solubilizing purposes.[24] Therefore, they can be harnessed for their dual activity. TSDs of the drug can be formulated using a hydrophilic carrier like poloxamer and a porous carrier like Neusilin US2, which will not only enhance the drug dissolution but also improve the bioabsorption by P-gp inhibition.[25] The tablets can then be coated using a pH-sensitive polymer, which will provide spatial and temporal control of drug delivery into the colonic region. This will limit the side effects of drugs associated with upper gastrointestinal tract.[26]

Materials and Methods

Rifaximin was a gratis sample from Amneal Pharmaceuticals, India. Gangwal Chemicals, India generously provided a sample of Neusilin US2. Eudragit S100 and Eudragit L100 were gift samples from Evonik India Ltd. Poloxamer 188, sodium lauryl sulfate (SLS), acetone, methanol, dimethyl sulfoxide, dimethyl formamide, ethanol, Avicel PH 102, and magnesium stearate were sourced from S.D. Finechem, India.

Methods

Analytical method

Rifaximin was analyzed by reverse-phase high-performance liquid chromatography (HPLC) (Agilent 1100, USA), using a Phenomenex C18 column (250 mm × 4.6 mm, 5 µm packing) at 25°C. The mobile phase comprised sodium acetate buffer: acetonitrile (60:40 v/v wherein the pH was set to 5.0 using 0.1N sodium hydroxide solution). The mobile phase was passed through the column at a 1.0 mL/min flow rate. UV detection was done at 293 nm and the retention peak of rifaximin was seen at 3.52 min.[27]

Preparation of rifaximin ternary solid dispersion

The TSD was prepared using the solvent evaporation technique. Rifaximin (crystalline) and poloxamer 188 were dissolved in acetone under stirring to form a solution. Neusilin US2 was dispersed in this solution of rifaximin and poloxamer 188, under stirring. The ratio of solvent: solid was kept constant at 1:5. Evaporation of acetone was done using a rotary vacuum evaporator (Super Techno Associates, India) at a temperature of 50°C under vacuum of 300 mmHg. Poloxamer 188 and Neusilin US2 were investigated in varying proportions. The optimization of TSD was based on dissolution enhancement and P-gp inhibition.[28]

Flow properties of TSD

To determine the flow properties of rifaximin TSD using a fixed height funnel method, the angle of repose (θ) was measured. Various parameters were also calculated using the following equations: bulk density, tapped density, Hausner's ratio, and Carr's index.[29-31]

$$\theta = \tan^{-1} h/r \quad (1)$$

$$\text{Bulk density} = \frac{\text{Mass of the blend}}{\text{Bulk volume of the cylinder}} \quad (2)$$

$$\text{Tapped density} = \frac{\text{Mass of the blend}}{\text{Tapped volume of the cylinder}} \quad (3)$$

$$\text{Hausner's ratio} = \frac{\text{Tapped density}}{\text{Bulk density}} \quad (4)$$

$$\text{Carr's index} = \frac{(\text{Tapped density} - \text{bulk density})}{\text{Tapped density}} \times 100 \quad (5)$$

Dissolution study of TSD

Dissolution of TSD was carried out by filling the TSD in a size 0 hard gelatin capsule using USP dissolution apparatus II at 75 rpm which was thermostatically kept at 37°C. The dissolution medium for the study was 900 mL, volume of 0.1 M sodium phosphate buffer, pH 7.4 with an additional 0.45% SLS. An aliquot of 5 mL of sample was removed at each 1-h interval till 6 h. The sample was filtered, diluted suitably, and analyzed by HPLC with UV detection at a wavelength of 293 nm. An aliquot of 5 mL of fresh media was replenished to compensate for the removed aliquot.[14]

Everted gut sac model for permeability assessment

Gut sac isolation and preparation

As previously reported, the everted gut sac method was used.[32] The study was performed in compliance with the Animal Ethics Committee-approved protocol BIP/IAEC/2019/09 and in adherence to the CPCSEA (Committee for the Purpose of Control and Supervision of Experiments on Animals) guidelines. The Wistar rats of either sex were made to fast overnight preceding the study with water *ad libitum*. The rats were humanely euthanized under a high dose of ketamine anesthesia. The intestinal segment was identified (starting 10 cm below the duodenum) and isolated. After flushing with cold saline, the intestinal section was stabilized in oxygenated Krebs-Ringer bicarbonate buffer having 10 mM glucose at 37°C; subsequently, the intestinal segment was gently everted with the help of a glass rod. One end of the intestinal section was tied using a thread to make a sac.[33]

Glucose transport across the everted gut sac

The glucose concentrations in the mucosal and serosal sides of the gut were measured to confirm the viability and the integrity of the gut; their ratios were calculated.[34] The incubation of sacs was in the presence of TSD in Krebs-Ringer bicarbonate buffer or absence of TSD (buffer only). The contents of the sacs and samples from the incubation medium were collected after 0, 30, 60, 90, and 120 min, collecting the serosal sample into Eppendorf tubes. Concentrations of glucose were assessed in a semi-automatic biochemical analyzer (Microlab Instruments, India).

Effects of TSD C5 on rifaximin transport across gut sac

In an incubation chamber, stabilized sacs were pre-incubated for 5 min with Krebs-Ringer bicarbonate buffer before being exposed to the test solution. Then, the sacs were incubated at 37°C, in a 50 mL oxygenated Krebs-Ringer bicarbonate buffer (pH between 7.0–7.2) containing rifaximin (crystalline) suspension/rifaximin TSD C5 suspension (equivalent to 25 µg/mL of rifaximin). Rifaximin suspension was prepared by dispersing the crystalline drug with 0.5% w/w carboxy methyl cellulose in distilled water. Under these conditions, the transport of rifaximin from mucosal to serosal side in each group was measured by removing the sac and draining the serosal fluid into Eppendorf tubes. A sampling of 50 µL of the serosal medium was done from the drained fluid at 0, 30, 60, 90, and 120 min. Prior to and post-serosal fluid collection, each sac was weighed to determine its volume and to correct the serosal fluid for the actual volume. All samples were quantified using HPLC. The apparent permeability coefficient (P_{app}) was calculated by the following formula:

$$P_{app} = \frac{(dQ/dt)}{(A \times C_0)}, \quad (6)$$

where dQ/dt is the rate of appearance of rifaximin in the everted gut sac (serosal side) (µg/s), A is the cross-sectional area of the intestinal section (cm^2), and C_0 is the initial concentration of rifaximin outside the everted gut sac (mucosal side) (µg/mL).[35,36]

Caco-2 permeability studies

Caco-2 (passage: 20–25) cells were acquired from the National Center for Cell Science (NCCS), Pune, India. Cells were cultured in supplemented Dulbecco's modified Eagle's medium in a moistened environment of 5% CO_2 at 37°C. After harvesting, the cells were grown on cell culture inserts for 21 days and the permeability studies started once the trans-epithelial electrical resistance value was ≥ 250 Ω cm^2. Hanks' balanced salt solution was supplemented with 25 mM HEPES and 10 mM D (+)-glucose; pH 7.4 was employed as a tra nsport medium for the studies. The apical-to-basolateral transport was studied for rifaximin (crystalline) suspension and rifaximin TSD C5 at a concentration of 25 µg/mL. An aliquot of 250 µL sample was added to the apical compartment and the basolateral compartment was filled with 800 µL of the transport medium. For basolateral-to-apical transport (BL→AP), the reverse configuration was employed wherein 800 µL samples were used basolaterally, whereas the apical compartment consisted of a 250 µL blank transport medium. Samples were removed at fixed time intervals of 15, 30, 60, 90, and 120 min and instantly substituted with an equal volume of transport medium.[37] P_{app} (AP → BL) and P_{app} (BL → AP) (apparent permeability coefficients in both directions) were estimated using equation (6). The terms in equation (6) are given as: P_{app} is the apparent permeability coefficient (cm/s), dQ/dt (µg/s) is the rate of permeation of rifaximin, A is the surface area of the monolayer, and C_0 is the initial concentration of rifaximin in the apical/basolateral sides (µg/mL). The efflux ratio was estimated by the following equation:

$$ER = \frac{P_{app}(BL\text{fi } AP)}{P_{app}(AP\text{fi } BL)}. \quad (7)$$

Characterization of TSD C5

Scanning electron microscopy

Morphological evaluation of rifaximin (crystalline), Neusilin US2, and rifaximin TSD C5 was carried out by scanning electron microscope with Oxford EDS system. The samples were fixed on aluminum stubs with the aid of double-sided adhesive tape before imaging. Using a high-vacuum evaporator and a gold sputter coater, they were gold-coated to a thickness of 250 Å and samples were analyzed by SEM.[38]

Differential scanning calorimetry

Differential scanning calorimetry (DSC) of rifaximin (crystalline), rifaximin-loaded Neusilin US2, and rifaximin TSD C5 was done using DSC-60 Shimadzu, Japan. Samples were analyzed with a scanning rate of 10°C/min, in the range of 50–350°C under nitrogen flushing (10 mL/min) at a temperature ramp rate of 10°C/min.[39]

X-ray diffraction

The X-ray diffraction (XRD) patterns of rifaximin (crystalline), rifaximin-loaded Neusilin US2, and rifaximin TSD C5 were documented employing the radiation at 30 kV and 25 mA, scanning speed at 20/min^{-1}, and 5–50 diffraction angle (2θ) ranges in a Rigaku Miniflex Diffractometer (Japan).[40]

FTIR

Rifaximin (crystalline), rifaximin-loaded Neusilin US2, and rifaximin TSD C5 were sealed in vials and kept at 50°C for 2 weeks. Rifaximin-loaded Neusilin US2 and rifaximin TSD C5 were evaluated for compatibility by ATR FTIR (Cary360, Agilent). The spectra were recorded from wave number 650 to 4000 cm^{-1}.[41]

Preparation of core tablets and post-compression characterization

Core tablets were prepared using a direct compression technique using rifaximin TSD (C5), Avicel PH102, and magnesium stearate as tablet excipients. Tablets were assessed for quality-defining characteristics such as hardness, weight variation, friability, and disintegration.

pH-sensitive coating of tablets

Tablet coating was accomplished in a conventional coating pan (Janki Impex, India). Tablet cores were pre-heated to about 40°C and the pH-sensitive coating solution (Eudragit S100/Eudrgit L100 combination in acetone) was filled in the spray gun and coated on the tablets till the target tablet weight gain was achieved according to the design matrix.[42] The initial weight and the weight of dried coated tablets were checked to determine the weight gain. The inlet temperature was kept at 50–60°C to maintain the product at a temperature of 45–50°C and the pan was rotated at 12–14 rpm.

Optimization of enteric coating of tablets by 32 factorial design

Several research groups have suggested that the Eudragit S100: Eudragit L100 ratio and amount of coating are known to influence the precise drug release in the colon.[42-44] A 3^2 factorial design was employed to design the coating of pH-sensitive polymer.[45] The design was used to evaluate the influence of independent variables—% coating (X_1), ratio of Eudragit S100: Eudragit L100 (X_2) on dependent variables—drug release at 2 h (Y_1) and drug release at 8 h (Y_2). The responses were analyzed by Design Expert Software 11.0.3.0 (Stat-Ease Inc., Minneapolis, MN, US). The design is recorded in Table 1.

According to the experimental design, the polynomial equation is as follows:

$$Y = b_0 + b_1X_1 + b_2X_2 + b_{12}X_{12} + b_{11}X_{12} + b_{22}X_{22}....., \quad (8)$$

where Y is the dependent or response variable, b_0 is the arithmetic mean response of all trials, and b_1 and b_2 are the estimated coefficients for the corresponding factors X_1 and X_2. It is the average result of a single factor being changed from a low level to a high level. b_{12} is the coefficient for the interaction term (X_1X_2) and it indicates the effect of simultaneous variation of both the factors. b_{11} and b_{22} are the coefficients for the polynomial term (X_{12}, X_{22}) which are higher-order terms indicative of non-linearity at higher levels. Optimization of the final formulation was based on the criteria to minimize the drug release at 2 h and constraint was set at not more than 10% and to maximize the drug release at 8 h and constraint was set at not less than 85%. The desirability function was employed for the optimization of the formulation.

Table 1: 3^2 Full factorial design for optimization of pH-sensitive coating of tablets

Independent variables/ factor	Levels			Response variable	Constraints
	Low Level (-1)	Middle level (0)	High level (+1)		
% Coating (X_1)	5	7.5	10	Y_1= % drug release at end of 2nd hour in 0.1 N HCl + 0.45% SLS	Not more than 10%
Ratio of Eudragit S100: Eudragit L100 (X_2)	1:2	1:1	2:1	Y_2 = % drug release at end of 8th hour in 0.1 M sodium phosphate buffer pH 7.4 + 0.45% SLS	Not less than 85%

Table 2: Characterization of drug release and flow properties of TSD

Formulation code	Rifaximin (%)	Neusilin US2 (%)	Poloxamer 188 (%)	% CDR (6 h) (*n*=3)	Angle of repose (*n*=3)	Carr's index (*n*=3)	Hausner ratio (*n*=3)
Rifaximin	100	—	—	32.5 ± 5.1	42.6 ± 3.4	23.4 ± 2.1	1.36 ± 0.12
C1	25	75	—	43.1 ± 3.4	27.3 ± 2.1	11.2 ± 1.5	1.09 ± 0.13
C2	25	70	5	54.4 ± 2.9	29.1 ± 2.4	15.7 ± 1.3	1.18 ± 0.11
C3	25	65	10	62.9 ± 4.8	30.5 ± 1.8	18.1 ± 1.5	1.22 ± 0.15
C4	25	60	15	78.3 ± 5.3	32.7 ± 2.3	19.1 ± 1.6	1.24 ± 0.12
C5	25	55	20	87.8 ± 3.5	34.8 ± 2.6	21.0 ± 1.4	1.27 ± 0.14

In-vitro dissolution study of pH-sensitive polymer-coated tablets

The dissolution study of pH-sensitive polymer-coated tablets was conducted using USP type II dissolution apparatus at 75 rpm maintained at 37°C. The dissolution medium employed in the study was 900 mL of 0.1N HCl pH 1.2 + 0.45% SLS for the first 2 h, followed by 0.1 M sodium phosphate buffer pH 7.4 containing 0.45% SLS. An aliquot of 5 mL of sample was removed at each 1-h interval for the total duration of 8 h. The solution was filtered, diluted suitably, and analysis was done by HPLC.[46]

Accelerated stability studies

The optimized formulation of rifaximin tablets was chosen for conducting accelerated stability studies in compliance with the International Conference on Harmonization (ICH) Q1A (R2) guidelines. The optimized batch was filled in high-density polyethylene (HDPE) bottles and kept in a stability chamber (CHM-10S, Remi Instruments Ltd, Mumbai, India) maintained at 40 ± 2°C/75 ± 5% RH for 6 months. The samples were withdrawn at 3 M intervals and analyzed for assay, hardness, and % CDR at 2 and 8 h.

Results

The TSD was prepared by the solvent evaporation technique. The optimization of the drug: carrier ratio is an important aspect that influences the dissolution enhancement of the drug by multifarious mechanisms. Crystalline rifaximin was loaded on mesoporous carrier Neusilin US2 in the absence of poloxamer 188 and along with poloxamer 188 [Table 2]. Dissolution of rifaximin (crystalline) as well as varying proportions of Neusilin US2 and poloxamer 188 are shown in Table 2. Rifaximin (crystalline) showed very less dissolution of around 32% in 6 h. The batch C1 was drug adsorbate on mesoporous carrier Neusilin US2 alone and displayed a drug release of around 43% in 6 h. The dissolution study of the batches C2–C5 indicated that as the quantity of hydrophilic polymer is increased in TSD, dissolution enhancement was observed. The drug dissolution reached more than 85% in 6 h with 20% of poloxamer 188 in TSD C5. Further increments of poloxamer 188 were not investigated as a higher proportion of poloxamer 188 in TSD retarded the flow properties beyond acceptable levels and raise tablet compression issues.

Table 3: Glucose concentration between serosal and mucosal side of the gut sac

Time (min)	Ratio (serosal to mucosal)	
	Control (buffer)	Rifaximin TSD C5
0	1	1
30	1.56 ± 0.39	1.44 ± 0.18
60	1.98 ± 0.52	1.89 ± 0.30
90	2.58 ± 0.58	2.45 ± 0.40
120	2.96 ± 0.46	3.10 ± 0.37

Table 4: Permeability of rifaximin and rifaximin TSD across the everted gut sac

Group	Drug transport amount (µg/120 min/10 cm-sac)	P_{app} (cm/s)
Rifaximin	5.512 ± 1.45	9.3×10^{-7}
Rifaximin TSD C2	11.38 ± 2.51	1.91×10^{-6}
Rifaximin TSD C3	13.43 ± 2.78	2.26×10^{-6}
Rifaximin TSD C4	17.65 ± 2.63	2.97×10^{-6}
Rifaximin TSD C5	23.45 ± 3.21	3.94×10^{-6}

The glucose transport studies on the gut sac were undertaken to assess the viability and metabolic functioning of the isolated tissues. The concentration ratios of glucose between the serosal side and mucosal side are shown in Table 3. It was found that the ratios were increasing and reached around 3.1 at 120 min for TSD C5. The presence of TSD did not influence glucose transport.

The results of the drug transport studies are shown in Table 4. Rifaximin (crystalline) displayed very low permeability with P_{app} of about 9.3×10^{-7} cm/s (drugs with P_{app} values $<5 \times 10^{-6}$ cm/s are classified as low permeability drugs). The conversion of the rifaximin to a TSD significantly improved its permeability with more than 4-fold improvement in permeability.

Rifaximin (crystalline) suspension and rifaximin TSD C5 were gauged for comparative intestinal permeability by Caco-2 cell monolayers. The permeability coefficients, mean P_{app} (AP → BL) of rifaximin (crystalline) suspension and rifaximin TSD C5, were $1.21 \pm 0.44 \times 10^{-6}$ and $5.84 \pm 0.34 \times 10^{-6}$ cm/s, respectively, which was significantly ($P < 0.01$) increased (4.83-folds) than rifaximin suspension [Table 5]. The observed mean P_{app} (BL→AP) values of rifaximin (crystalline) suspension and rifaximin TSD C5 were

$4.50 \pm 0.28 \times 10^{-5}$ and $8.96 \pm 0.48 \times 10^{-5}$ cm/s, respectively. The P-gp efflux ratios of rifaximin (crystalline) suspension and rifaximin TSD were 37.19 and 15.34, respectively.

The surface morphology of the rifaximin (crystalline) shows the presence of irregular crystals of the rifaximin in the SEM micrograph [Figure 1(a)]. SEM of Neusilin US2 [Figure 1(b)] shows its porous and spherical structure. SEM of TSD C5 [Figure 1(c)] indicates that when rifaximin (crystalline) and Poloxamer 188 are loaded on Neusilin US2, the crystallinity of the rifaximin is lost and no agglomeration is visible.

DSC thermograms of rifaximin (crystalline), rifaximin-loaded Neusilin US2, and rifaximin TSD C5 are shown in Figure 2. DSC thermogram of rifaximin (crystalline) showed an endothermic peak at 226.63˚C which corresponded to its melting point. This DSC thermogram showed broadening of endotherms with rifaximin-loaded Neusilin US2 and rifaximin TSD C5.

XRD spectra of rifaximin (crystalline) [Figure 3(a)] exhibit sharp peaks at 2θ 6.79, 7.67, 10.23, 18.08, 18.26. XRD patterns of rifaximin-loaded Neusilin US2 and rifaximin TSD C5 [Figure 3(b) and (c)] show the absence of characteristic peaks of rifaximin and display a diffused pattern.

The FTIR spectra of rifaximin (crystalline), rifaximin-loaded Neusilin US2, and rifaximin TSD C5 are shown in Figure 4. The FTIR spectra displayed sharp peaks of the characteristic groups: C=0, C = N, O-H, aliphatic C-H stretch, and C = C aromatic.

Rifaximin TSD C5 was selected as optimized batch of TSD based on dissolution enhancement, processing ease,

Table 5: *In-vitro* permeability study of rifaximin suspension and rifaximin TSD

Rifaximin (crystalline) suspension		Rifaximin TSD C5		Efflux ratio	
AP-BL	BL-AP	AP-BL	BL-AP	Rifaximin-suspension	Rifaximin TSD C5
$1.21 \pm 0.44 \times 10^{-6}$ cm/s	$4.50 \pm 0.28 \times 10^{-5}$ cm/s	$5.84 \pm 0.34 \times 10^{-6}$ cm/s	$8.96 \pm 0.48 \times 10^{-5}$ cm/s	37.19	15.34

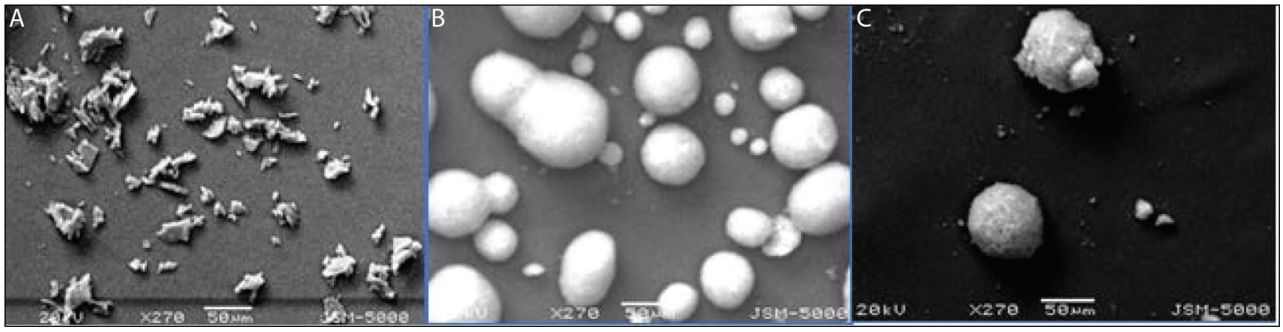

Figure 1: (a) SEM of rifaximin (crystalline), (b) SEM of Neusilin US2, and (c) SEM of rifaximin TSD C5

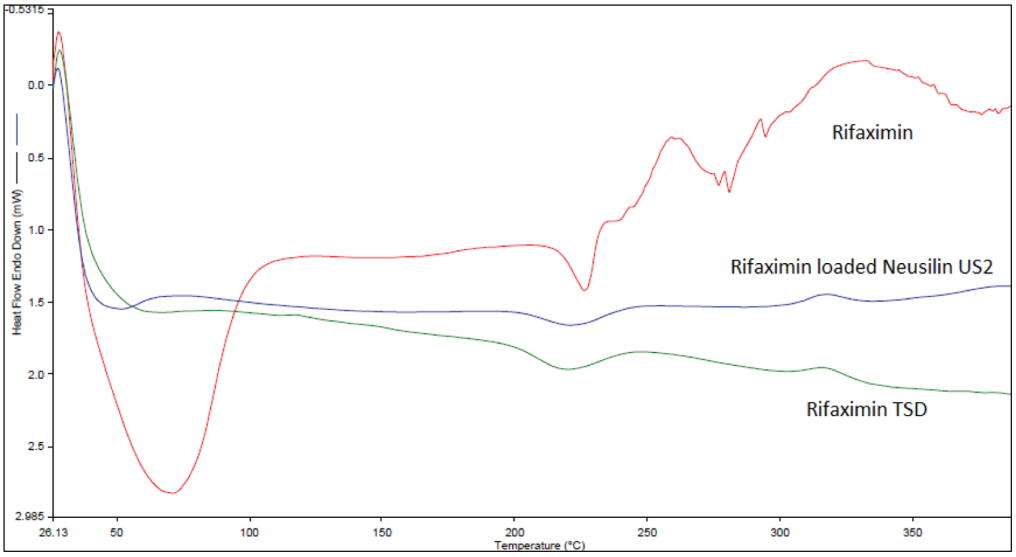

Figure 2: DSC thermograms of rifaximin, rifaximin-loaded Neusilin US2, and rifaximin TSD C5

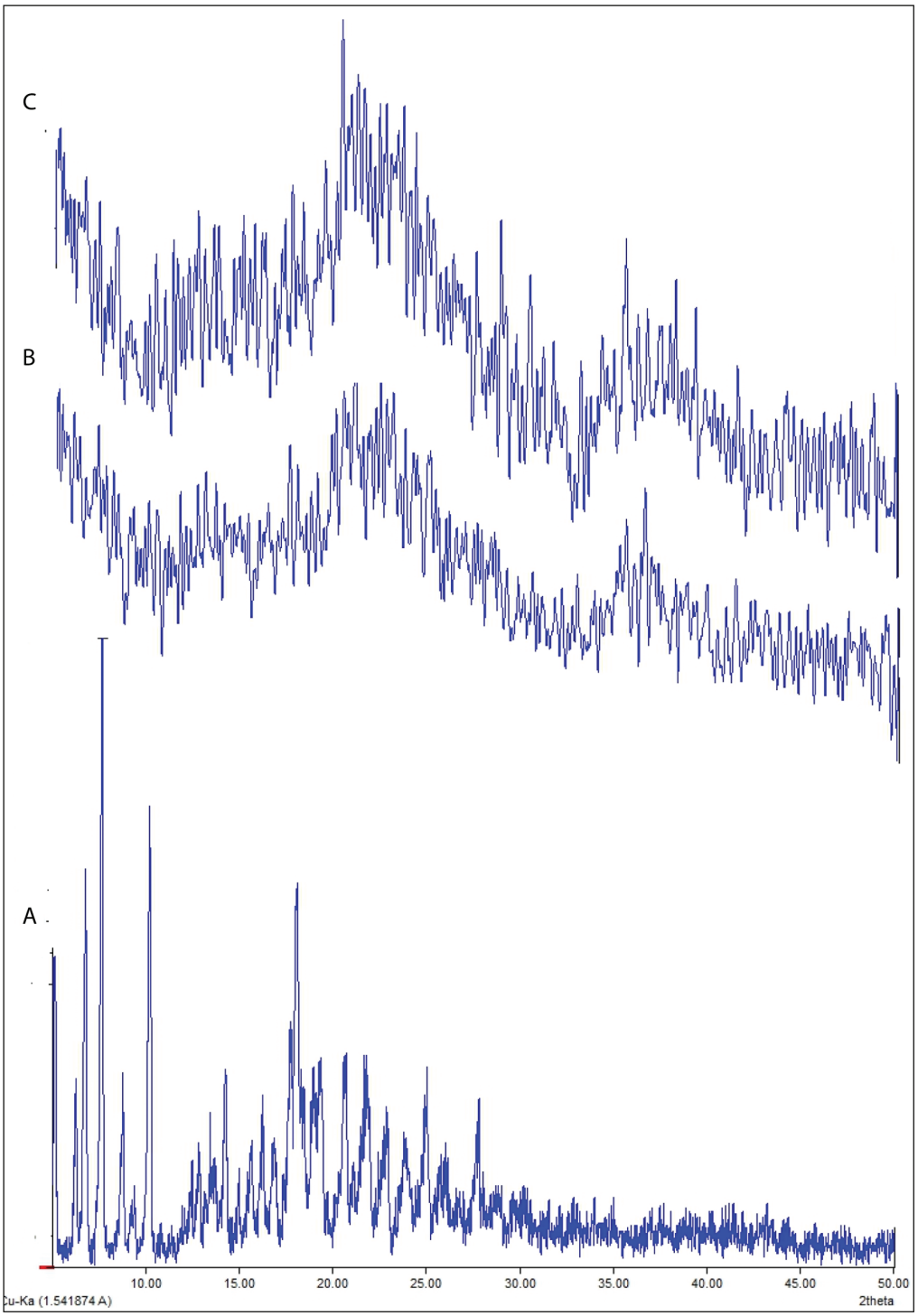

Figure 3: (a) XRD spectra of rifaximin, (b) XRD of rifaximin-loaded Neusilin US2, and (c) XRD of rifaximin TSD C5

and permeability enhancement. Optimized rifaximin TSD C5 was blended with excipients and the tablet blend was subjected to the standard precompression evaluations. Carr's index was 21.51 ± 1.61 and the angle of repose was 33.5 ± 1.11. Core tablets were assessed for post-compression parameters at the pre-coating stage and post-coating with pH-sensitive Eudragit coating [Tables 6 and 7]. The physical examination of the tablets revealed that they were devoid of any physical defects and passed the tests for thickness, diameter, weight variation, and friability. The hardness of the uncoated tablet was 9.3 kg/cm^2, whereas that of the coated tablet was 10.4 kg/cm^2. Both the coated and uncoated tablets had an assay of greater than 98%.

A 3^2 factorial design was used to characterize the influence of independent variables, % coating (X_1), ratio of Eudragit S100: Eudragit L100 (X_2) on dependent variables, drug

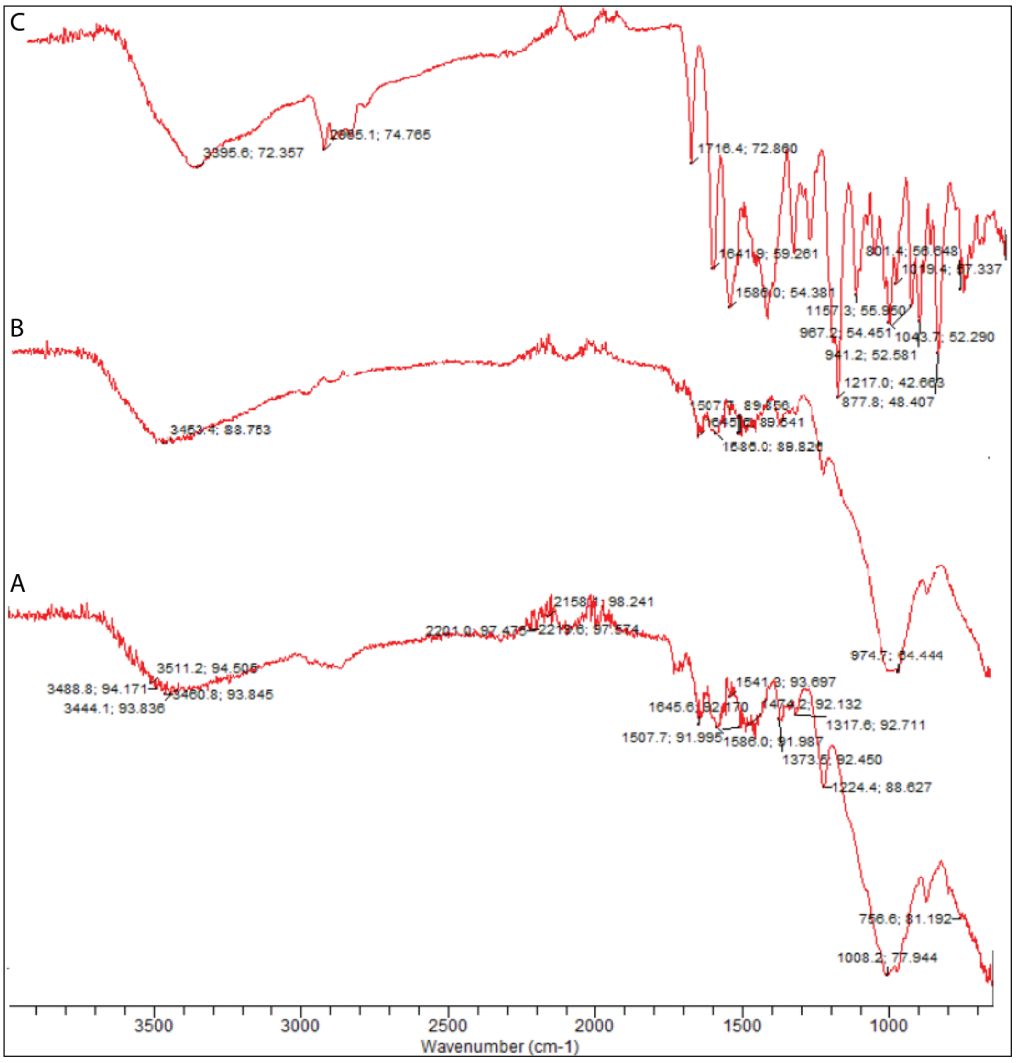

Figure 4: (a) FTIR spectra of rifaximin, (b) FTIR spectra of rifaximin-loaded Neusilin US2, and (c) FTIR spectra of rifaximin TSD C5

Table 6: Pre-compression and post-compression parameters of TSD C5 tablet blend/core tablets

Parameter	Result
Bulk density (g/cc)	0.124 ± 0.09
Tapped density (g/cc)	0.158 ± 0.05
Hausner's ratio	1.27 ± 0.22
Carr's index	21.51 ± 1.61
Angle of repose (°)	33.5 ± 1.11
Drug content (%)	98.34 ± 2.81
Average weight (mg)	822 ± 4.1
Hardness (kg/cm^2)	9.3 ± 2.64
Friability (%)	0.56 ± 0.18

Table 7: Composition and characterization of optimized formulation of pH-sensitive polymer-coated tablets

Rifaximin TSD C5 equivalent to 200 mg of rifaximin (mg)	800
Magnesium stearate (mg)	8.0
Avicel pH 102 (mg)	q.s. to 820
Average tablet weight (mg)	822 ± 4.1
% Coating	5.06
Ratio of Eudragit S100: L100	1.3:1.7
Coated tablet weight (mg)	861.2 ± 6.05
Hardness (kg/cm^2)	10.4 ± 0.59
Friability (%)	0.39 ± 0.15
% Drug content	98.48 ± 1.28
Drug release at 2 h (%)	3.09 ± 0.97
Drug release at 8 h (%)	96.2 ± 2.39

release at 2 h (acid phase) (Y_1), and drug release at 8 h (basic phase) (Y_2). Dissolution was carried out in 0.1 N HCl + 0.45% SLS for 2 h to account for the acid stage in the stomach. It was followed by a release study in 7.4 pH phosphate buffer + 0.45% SLS for 6 h. Table 8 depicts the design matrix and responses observed for the experimental batches. The contour plot and 3D response surface plot to map the effect of independent variables on response, i.e., drug release at 2 h, are shown in Figur 5. The fit summary for the statistical model suggested a linear model. The R^2 value was found to be 0.9838. The

Table 8: Design matrix and response in 3^2 full factorial design for optimization of pH-sensitive coating

Batch no.	Response					
	Coded value		Uncoded value		% DR at 2 h (n=6)	% DR at 8 h (n=6)
	X_1	X_2	X_1	X_2		
AB1	-1	-1	5	1:2	3.41 ± 0.4	97.6 ± 4.5
AB2	0	-1	7.5	1:2	2.36 ± 0.3	91.2 ± 3.6
AB3	1	-1	10	1:2	1.02 ± 0.3	92.9 ± 2.8
AB4	-1	0	5	1:1	2.71 ± 0.6	95.3 ± 4.1
AB5	0	0	7.5	1:1	1.88 ± 0.5	90.2 ± 3.3
AB6	1	0	10	1:1	1.2 ± 0.4	88.5 ± 2.6
AB7	-1	1	5	2:1	2.35 ± 0.5	82.7 ± 2.3
AB8	0	1	7.5	2:1	1.46 ± 0.3	79.2 ± 2.9
AB9	1	1	10	2:1	1.1 ± 0.2	75.2 ± 2.1
Statistical constants		Drug release at 2 h			Drug release at 8 h	
Model P-value		<0.0001			0.0055	
Model F-value		79.90			42.34	
Adjusted R^2		0.9518			0.9627	
Predicted R^2		0.9309			0.8299	
Adequate precision		23.239			17.854	
C.V. (%)		4.85			1.65	

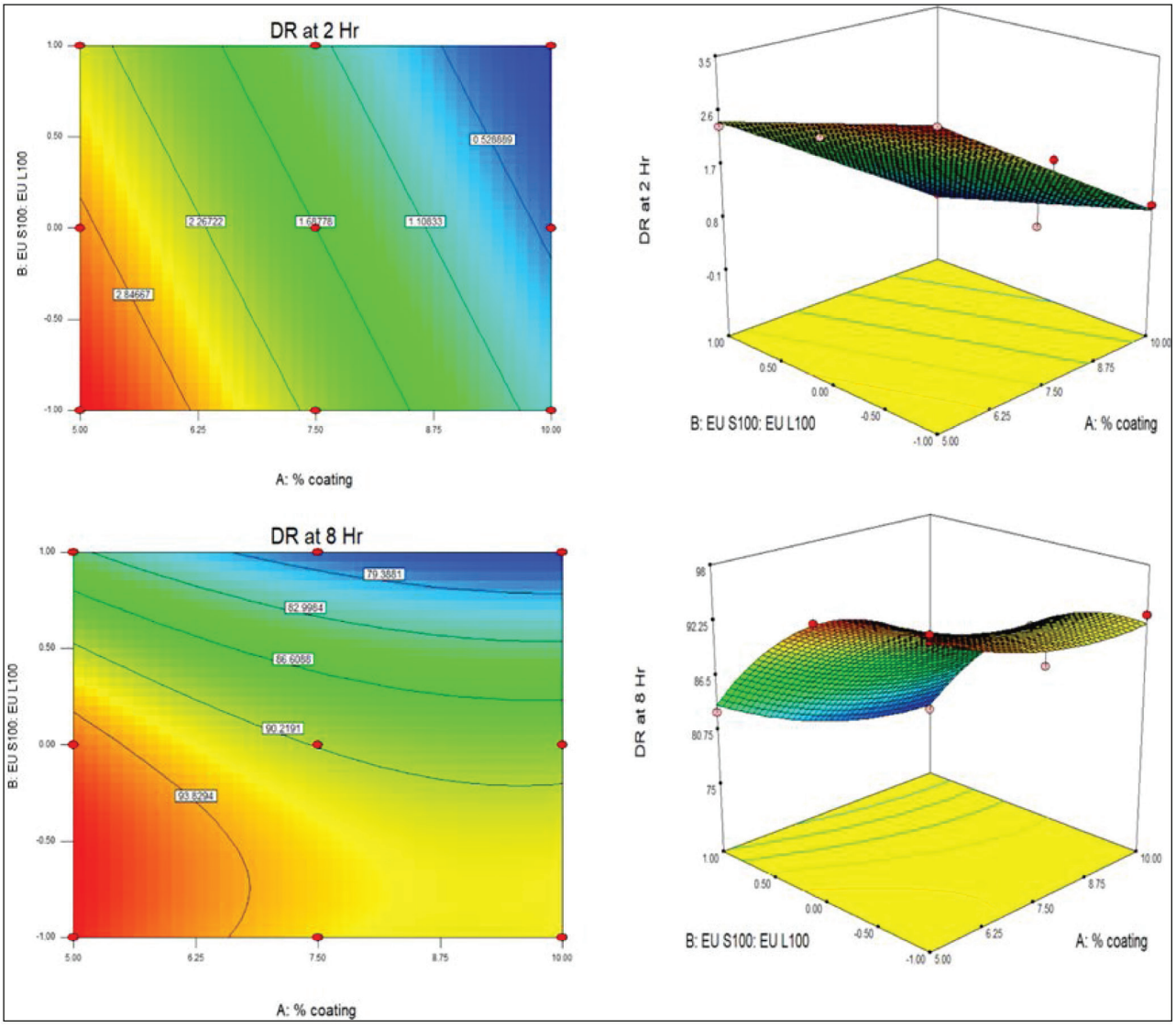

Figure 5: Contour plot and 3D surface plot of effect of formulation on drug release at 2 and 8 h

F-value was found to be 79.90 implying that the model was significant [Table 8]. The polynomial equation gives the mathematical relationship between the independent and dependent variables. Both X_1 and X_2 had a significant bearing on the drug release at 2 h. The equation indicates the absence of any interaction and higher-order effects and is an equation of a linear model. It was observed that a combination of Eudragit S100 and L100 can restrict the drug release to below 10% in acidic media in all the investigated combinations [Table 8].

$$Y_1 = 1.69 - 1.24 * X_1 - 0.50 * X_2.$$

The relationship between independent variables and the dependent variable—drug release at the end of 8 h was found to be quadratic. The fit summary for the statistical model suggested a quadratic model. The R^2 value was found to be 0.9860. The *F*-value was found to be 42.34 implying the significance of the model [Table 8]. Both the independent variables were significant and their interaction and higher-order effects were also found to be influencing the response variable.

$$Y_2 = +90.11 - 3.17 * X_1 - 7.43 * X_2 - 0.70 * X_1 * X_2 + 1.83 X_{12} - 4.87 X_{22}.$$

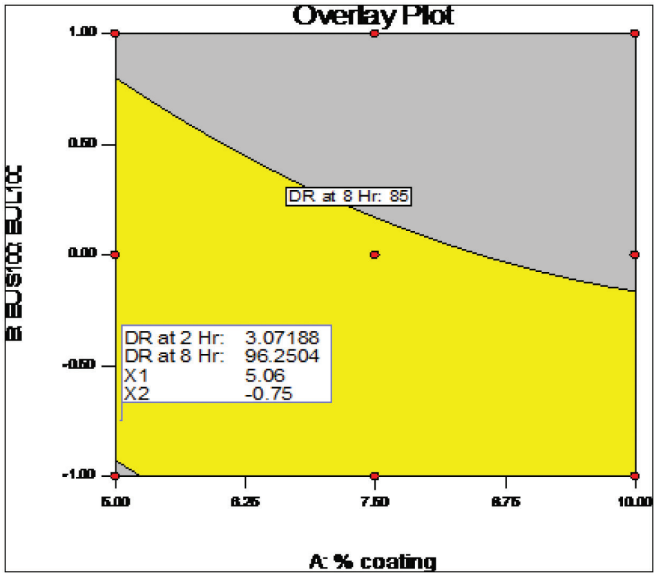

Figure 6: Overlay plot for formulation optimization

The optimization of the formulation was done by the numerical and graphical method using the overlay region [Figure 6] and desirability (*D*) values. The desirable yellow region was obtained by applying the constraints to variables. Numerical optimization based on the desirability function yielded the best fitting solutions. From the solutions provided by the software, the batch with the highest desirability was selected as the optimized batch. The final batch had a coating of 5% and with a combination of Eudragit S 100:Eudragit L100 at a ratio of 1.3:1.7. The optimized batch was prepared according to the procedure specified earlier and characterized for the post-compression parameters and drug release studies [Table 7].

The stability studies conducted at accelerated conditions of 40 ± 2°C/75 ± 5% RH for 6 months did not show any statistically significant difference [Table 9]. The parameters continued to be within acceptable limits indicating the stability of the developed dosage form.

Discussion

The TSD was prepared by the solvent evaporation technique and optimized for a rifaximin: neusilin US2 ratio. Rifaximin is a BCS class IV drug and hence, the drug showed very less dissolution. The inclusion of rifaximin in mesoporous carrier Neusilin US2 (C1) alone leads to an increase in the dissolution, which is insufficient. This shows that drug adsorption alone on the mesoporous carrier may not suffice to show satisfactory dissolution and consequent bioavailability enhancement. This warrants the need of a hydrophilic polymer that can be incorporated to produce a TSD. Poloxamer 188 as a hydrophilic carrier and surfactant aids in solubility enhancement to achieve desired dissolution profile is well reported in the literature. Further, poloxamer is also reported to be a P-gp inhibitor and can improve the permeation of P-gp substrate drugs. The low bioavailability of rifaximin is also attributable to both low solubility and P-gp efflux mechanism. Hence, it was decided to include poloxamer 188 in TSD to harness its dual benefits as a hydrophilic polymer to improve the dissolution and as P-gp inhibitor in TSD formulation.[47]

It is observed that the drug, hydrophilic polymer, must be loaded effectively in the mesoporous structure of the carrier to be valuable in demonstrating dissolution

Table 9: Stability data of the developed (TSD C5 enteric-coated tablets) formulation

Stability condition: 40 ± 2°C/75 ± 5% RH			
Pack: HDPE bottles (30 mL)			
Test	**Initial**	**3 months**	**6 months**
Description	**White to off-white, flat-faced, circular tablets**	**White to off-white, flat-faced, circular tablets**	**White to off-white, flat-faced, circular tablets**
Assay (%)	98.48 ± 1.28	96.3 ± 2.81	97.1 ± 3.3
Hardness (kg/cm^2)	10.4 ± 0.59	10.6 ± 0.4	11.1 ± 0.9
Drug release at 2 h	3.09 ± 0.97	2.54 ± 1.2	4.6 ± 0.7
Drug release at 2 h	96.2 ± 2.39	94.4 ± 3.9	93.1 ± 2.8

improvement. The dissolution study reflected clearly that increasing the quantity of hydrophilic polymer in TSD enhances the dissolution significantly. The dissolution enhancement can be attributed to not only the solid dispersion properties like molecular dispersion of API and improved wetting but also the increased surface area due to the use of adsorption carriers. It is reported that the inclusion and adsorption on carrier lead to nano-confinement of drug and/or drug-hydrophilic polymer—Neusilin complex formation by acid–base reaction, ion–dipole interactions, hydrogen bonding, and so on. Studies by researchers have shown that the inclusion of drug solid dispersions in the mesoporous carriers helps to stabilize the amorphous form of the drug and prevent the reversion to crystalline form. The DSC and XRD study results were also concurrent to the above argument. These multimodal mechanisms can in consequence bring about the dissolution enhancement and are expected to increase bioabsorption of the drug.[48,49]

The glucose transport studies on the gut sac are a good measure to reflect upon the relevance of the studies performed using isolated tissues. The glucose ratios increased steadily over 2 h and were similar for the control group and the TSD, implying that the presence of TSD did not influence the glucose transport. This is indicative of a viable gut sac and the absence of any significant effect of TSD on viability and energy-related processes.[35,36]

The TSD C5 of the drug markedly enhanced the permeability characteristics. The presence of poloxamer 188 in TSD C5 not only aided in dissolution but also enhanced the permeability by inhibiting the P-gp efflux transport of the rifaximin. Rifaximin permeability is reported to change 2–12 folds when co-administered with a P-gp inhibitor. The gut sac studies showed a nearly 5-fold augmentation in permeability of rifaximin from TSD C5. The inferences of gut sac studies were further corroborated with Caco-2 permeability studies. The dual directional (AP → BL and BL → AP) transport analysis in the Caco-2 monolayer is exceptionally useful for the evaluation of substrates and inducers/inhibitors of P-gp transporters. The plausible reason for enhanced transepithelial permeability with rifaximin TSD could be attributed to improved dissolution as well as inhibition of p-gp efflux. Efflux ratios of the drug are an indication of the net efflux transport. Efflux ratio with rifaximin TSD C5 is significantly decreased to one-third of that observed with rifaximin (crystalline) suspension. A marked change was seen in the fluxes of the rifaximin from the basolateral side to the apical side in comparison to the flux from the apical side to the basolateral side, confirming the role of active efflux mechanism and need for addressing it. The secretory effect of rifaxmin (crystalline) suspension was higher than the absorptive effect.[37]

SEM micrographs showed the crystallinity of rifaximin and mesoporous structure of Neusilin US2, which is reported to provide a large surface area for adsorption. The porous and spherical structure of Neusilin US2 can account for the drug loading as well as the excellent flow properties of the adsorbate. SEM of TSD C5 indicated a loss of crystallinity of rifaximin attributable to the TSD formation and inclusion in the porous structure.[50]

DSC thermogram of rifaximin shows an endothermic peak at 226.63°C, which corresponds to its melting point and reflects its crystallinity. These broadened peaks in DSC thermograms of rifaximin-loaded Neusilin US2 and rifaximin TSD C5 indicated the transformation of the rifaximin (crystalline) into an amorphous form.[51]

XRD spectra of rifaximin (crystalline) exhibited sharp peaks at 2θ 6.79, 7.67, 10.23, 18.08, 18.26, which specifies its crystalline nature. XRD spectra of rifaximin-loaded Neusilin US2 and rifaximin TSD C5 [Figure 3(b) and (c)] show the absence of sharp peaks of crystalline rifaximin and are indicative of an amorphous form. Thus, these complementary studies confirm that conversion of a rifaximin from its crystalline to amorphous state occurs due to TSD formation, adsorption over the porous carrier, and resulting in a consequent increase in dissolution.[52]

The FTIR spectra of rifaximin (crystalline), rifaximin-loaded Neusilin US2, and rifaximin TSD C5 [Figure 4] are indicative of the characteristic functional groups of the rifaximin. Some of the characteristic peaks of rifaximin (crystalline) have disappeared or broadened in FTIR spectra of rifaximin-loaded porous carrier and TSD due to probable hydrogen bonding with Neusilin US2. It has been reported that silanol groups present on the surface of the Neusilin are capable of hydrogen bonding with drugs, resulting in the FTIR peak broadening.[53,54]

Pre-compression assessment on the tablet blend indicated good flow properties and compressibility, and thus blend can be considered suitable for high-speed compression. Direct compression is the highly preferred method of tablet manufacturing as it saves time due to a lower number of manufacturing steps. Core tablets and coated tablets were assessed for post-compression parameters which were all in the desirable range. The rifaximin content in core and coated tablets was more than 98%, indicating that the processing did not cause any loss or instability of the drug.

Statistical DOE technique and response surface methodology were employed to optimize the coating composition. Literature has revealed that the nature of pH-sensitive polymer and % coating are the major parameters affecting drug release from coated formulations. By predicting how the dosage form will release the drug, one can gain insight into the delivery system's *in-vivo* behavior. Eudragit S100, Eudragit L100, and their combination have been maximally explored for colon targeting.[43] With reference to prior knowledge, different ratios of Eudragit S100 and Eudragit L100 and % coating varying between 5% and 10% were

explored during optimization studies. A 3^2 experimental design explores two independent variables at three different levels so that optimized combination of variables can be utilized for desirable outcomes of dependent variables. The polynomial equation generated by the software aids in establishing a mathematical model for the independent and dependent variables. It was observed in the studies that all the batches could restrict the drug release in the acidic media below 10%, meeting the desirability criteria. The mathematical model suggested the influence of both parameters, viz., coating % and ratio of the polymers in restricting the drug release in acidic media. The chosen range of both variables in all possible combinations was effective in restraining the rifaximin release in an acidic environment. Hence, the major response variable in optimizing the pH-sensitive coating was drug release at 8 h in the buffer media. It was observed that both the independent variables were significant and their interaction and higher-order effects were also found to be influencing the response variable. The response plot showed that as % coating reduced, the drug release from the tablets increased. The higher proportion of the S100 leads to the slower dissolution of enteric coating in the buffer media. The criterion for optimization was maximizing the drug release and the limit was affixed to not less than 85% drug release at the end of 8 h. For both the response variables, the *P*-values indicated that lack-of-fit was trivial and the residuals revealed the validity of the underlying assumptions. Furthermore, $P < 0.05$ for the model implied the significance of the developed model. The influence of both factors, i.e., polymer ratio and % coating, was relatively larger for Y_2 as pointed out by higher numerical values of the coefficient for Y_2 in comparison to Y_1. Numerical and graphical optimization generated the best fitting solutions. The software-generated solution was formulated and assessed which m*et al*l the criteria of drug release and other post-compression characteristics. The drug release was less than 5% in 2 h and more than 95% after 6 h in buffer media.[16]

Conclusion

The studies explored the possibility of using Poloxamer 188 as P-gp inhibitor and dissolution enhancer for BCS class IV drugs. The solid dispersion on adsorption on a mesoporous carrier not only enhanced processibility of the formulation but also aided in enhanced dissolution by stabilized amorphization of the drug. The use of P-gp inhibitor in the formulation can be harnessed to achieve higher permeation across Caco-2 cell lines and inhibit the efflux of drug. This is expected to translate to markedly improved bioabsorption of the drug *in vivo*. The pH-sensitive coating controlled dissolution of the drug in the colonic pH and might help in temporal as well as spatial control over the drug release in the colonic region *in vivo*. The studies conclusively present the TSD approach as an economically viable and effective resolution approach for poorly soluble and P-gp substrate drugs.

Acknowledgement

None.

Financial support and sponsorship

Nil.

Conflicts of interest

There are no conflicts of interest.

Authors' contributions

MSL: conception, interpretation of work, and final approval, PJS: critical revision for intellectual content, RK: drafting of article, HPP: drafting of article.

Ethical approval

The animal study was reviewed and approved by the Institutional Animal Ethics Committee of the Babaria Institute of Pharmacy.

Data availability statement

All datasets generated for this study are included in the article.

Consent for publication

All authors contributed to the article and approved the submitted version of research work in *Journal of Reports in Pharmaceutical Sciences*.

References

1. Rubin DC, Shaker A, Levin MS. Chronic intestinal inflammation: Inflammatory bowel disease and colitis-associated colon cancer. Front Immunol 2012;3:107.
2. Bouma G, Strober W. The immunological and genetic basis of inflammatory bowel disease. Nat Rev Immunol 2003;3:521-33.
3. Saha L. Irritable bowel syndrome: Pathogenesis, diagnosis, treatment, and evidence-based medicine. World J Gastroenterol 2014;20:6759-73.
4. Atreya I, Atreya R, Neurath MF. NF-κB in inflammatory bowel disease. J Intern Med 2008;263:591-6.
5. Botoman VA, Bonner GF, Botoman DA. Management of inflammatory bowel disease. Am Fam Physician 1998;57:57-68, 71-2.
6. Nitzan O, Elias M, Peretz A, Saliba W. Role of antibiotics for treatment of inflammatory bowel disease. World J Gastroenterol 2016;22:1078-87.
7. Viscomi GC, Campana M, Barbanti M, Grepioni F, Polito M, Confortini D, *et al*. Crystal forms of rifaximin and their effect on pharmaceutical properties. CrystEngComm 2008;10:1074-81.
8. DuPont HL. Biologic properties and clinical uses of rifaximin. Expert Opin Pharmacother 2011;12:293-302.
9. Mencarelli A, Migliorati M, Barbanti M, Cipriani S, Palladino G, Distrutti E, *et al*. Pregnane-X-receptor mediates the anti-inflammatory activities of rifaximin on detoxification pathways in intestinal epithelial cells. Biochem Pharmacol 2010;80:1700-7.
10. Zuo T, Ng SC. The gut microbiota in the pathogenesis and therapeutics of inflammatory bowel disease. Front Microbiol 2018;9:2247.
11. Scarpignato C, Pelosini I. Rifaximin, a poorly absorbed antibiotic: Pharmacology and clinical potential. Chemotherapy 2005;51(Suppl. 1):36-66.

12. Adachi JA, DuPont HL. Rifaximin: A novel nonabsorbed rifamycin for gastrointestinal disorders. Clin Infect Dis 2006;42:541-7.
13. Beig A, Fine-Shamir N, Lindley D, Miller JM, Dahan A. Advantageous solubility-permeability interplay when using amorphous solid dispersion (ASD) formulation for the BCS class IV P-gp substrate rifaximin: Simultaneous increase of both the solubility and the permeability. AAPS J 2017;19: 806-13.
14. Karanje RV, Bhavsar YV, Jahagirdar KH, Bhise KS. Formulation and development of extended-release micro particulate drug delivery system of solubilized rifaximin. AAPS PharmSciTech 2013;14:639-48.
15. Kumar J, Newton A. Colon targeted rifaximin nanosuspension for the treatment of inflammatory bowel disease (IBD). Antiinflamm Antiallergy Agents Med Chem 2016;15:101-17.
16. Nicholas ME, Prabakaran L, Sarkar S. A pragmatic approach on colonic delivery of rifaximin using polymer coated multi-particulate system. Int J Pharm Sci Res 2016;7:2465.
17. Rawoof MD, Rajnarayana K, Ajitha M. Formulation and evaluation of pH-dependent colon-targeted tablets of rifaximin by design of experiment. Asian J Pharm Clin Res 2019;12:249-54.
18. Kumar J, Newton AM. Rifaximin-chitosan nanoparticles for inflammatory bowel disease (IBD). Recent Pat Inflamm Allergy Drug Discov 2017;11:41-52
19. Zeeshan M, Ali H, Khan S, Khan SA, Weigmann B. Advances in orally-delivered pH-sensitive nanocarrier systems: An optimistic approach for the treatment of inflammatory bowel disease. Int J Pharm 2019;558:201-14.
20. Ulbrich W, Lamprecht A. Targeted drug-delivery approaches by nanoparticulate carriers in the therapy of inflammatory diseases. J R Soc Interface 2010;7(Suppl. 1):S55-66.
21. Argade P, Patole VC, Pandit AP. Liquisolid compact tablet of candesartan cilexetil with enhanced solubility using Neusilin US2, Aerosil 200 and Transcutol HP. Indian J Pharm Educ Res 2019;53:457-67.
22. Ahuja G, Pathak K. Porous carriers for controlled/modulated drug delivery. Indian J Pharm Sci 2009;71:599-607.
23. Rege BD, Kao JP, Polli JE. Effects of nonionic surfactants on membrane transporters in Caco-2 cell monolayers. Eur J Pharm Sci 2002;16:237-46.
24. Neha S, Meenakshi B. Solubility enhancement technique: A review. Int J Pharm Erud 2011;1:40-53.
25. Vojinović T, Medarević D, Vranić E, Potpara Z, Krstić M, Djuriš J, *et al*. Development of ternary solid dispersions with hydrophilic polymer and surface adsorbent for improving dissolution rate of carbamazepine. Saudi Pharm J 2018;26:725-32.
26. Qureshi AM, Momin M, Rathod S, Dev A, Kute C. Colon targeted drug delivery system: A review on current approaches. Indian J Pharm Biol Res 2013;1:130-47.
27. Sumakala S, Surendran V, Dharani NR. Development and validation of stability indicating RP-HPLC method for estimation of rifaximin in bulk and formulation. Int J Adv Res 2016;4:200-7.
28. Afifi S. Solid dispersion approach improving dissolution rate of stiripentol: A novel antiepileptic drug. Iran J Pharm Res 2015;14:1001-14.
29. Govedarica B, Injac R, Srcic S. Formulation and evaluation of immediate release tablets with different types of paracetamol powders prepared by direct compression. Afr J Pharmacy Pharmacol 2009;5:31-41.
30. Ganesan V, Rosentrater KA, Muthukumarappan K. Flowability and handling characteristics of bulk solids and powders—A review with implications for DDGS. Biosyst Eng 2008;101:425-35.
31. Saker A, Cares-Pacheco MG, Marchal P, Falk V. Powders flowability assessment in granular compaction: What about the consistency of Hausner ratio? Powder Technol 2019;354:52-63.
32. Yumoto R, Murakami T, Nakamoto Y, Hasegawa R, Nagai J, Takano M. Transport of rhodamine 123, a P-glycoprotein substrate, across rat intestine and caco-2 cell monolayers in the presence of cytochrome P-450 3a-related compounds. J Pharmacol Exp Ther 1999;289:149-55.
33. Shah P, Chavda K, Vyas B, Patel S. Formulation development of linagliptin solid lipid nanoparticles for oral bioavailability enhancement: Role of P-gp inhibition. Drug Deliv Transl Res 2021;11:1166-85.
34. Ballent M, Lifschitz A, Virkel G, Sallovitz J, Lanusse C. Modulation of the P-glycoprotein-mediated intestinal secretion of ivermectin: *In vitro* and *in vivo* assessments. Drug Metab Dispos 2006;34:457-63.
35. Li M, Si L, Pan H, Rabba AK, Yan F, Qiu J, *et al*. Excipients enhance intestinal absorption of ganciclovir by P-gp inhibition: Assessed *in vitro* by everted gut sac and *in situ* by improved intestinal perfusion. Int J Pharm 2011;403:37-45.
36. Parsa A, Saadati R, Abbasian Z, Azad Aramaki S, Dadashzadeh S. Enhanced permeability of etoposide across everted sacs of rat small intestine by vitamin E-TPGS. Iran J Pharm Res 2013;12:37-46.
37. Yadav M, Sarolia J, Vyas B, Lalan M, Mangrulkar S, Shah P. Amalgamation of solid dispersion and melt adsorption technique: Improved *in vitro* and *in vivo* performance of ticagrelor tablets. AAPS PharmSciTech 2021;22:257.
38. Pilli R, Nagabhushanam MV, Kadali SK. Etodolac dissolution improvement by preparation of solid dispersions with cyclodextrin complex's. Int J Pharm Sci Res 2014;5:4774.
39. Kogawa AC, Salgado HRN. Status of rifaximin: A review of characteristics, uses and analytical methods. Crit Rev Anal Chem 2018;48:459-66.
40. Zhao YM, Zheng ZB, Li S. Quantification of flupirtine maleate polymorphs using X-ray powder diffraction. Chin Chem Lett 2016;27:1666-72.
41. Deshmukh R, Harwansh RK. Preformulation considerations development and evaluation of mesalamine loaded polysaccharide-based complex mucoadhesive beads for colon targeting. Indian J Pharm Educ Res 2021;55:95-106.
42. Bando H, McGinity JW. Relationship between drug dissolution and leaching of plasticizer for pellets coated with an aqueous Eudragit® S100: L100 dispersion. Int J Pharmaceut 2006;323: 11-7.
43. Khan MZ, Prebeg Ž, Kurjaković N. A pH-dependent colon targeted oral drug delivery system using methacrylic acid copolymers: I. Manipulation of drug release using Eudragit® L100-55 and Eudragit® S100 combinations. J Control Release 1999;58:215-22.
44. Khan MZ, Stedul HP, Kurjaković N. A pH-dependent colon-targeted oral drug delivery system using methacrylic acid copolymers. II. Manipulation of drug release using Eudragit L100 and Eudragit S100 combinations. Drug Dev Ind Pharm 2000;26:549-54.
45. Kumria R, Al-Dhubiab BE, Shah J, Nair AB. Formulation and evaluation of chitosan-based buccal bioadhesive films of zolmitriptan. J Pharm Innov 2018;13:133-43.

46. Kogawa AC, Salgado HR. Evaluation of dissolution of rifaximin and its importance. Eur Chem Bull 2017;6:359-64.
47. Gurjar R, Chan CYS, Curley P, Sharp J, Chiong J, Rannard S, *et al*. Inhibitory effects of commonly used excipients on P-glycoprotein *in vitro*. Mol Pharm 2018;15:4835-42.
48. Azad M, Moreno J, Davé R. Stable and fast-dissolving amorphous drug composites preparation via impregnation of Neusilin® UFL2. J Pharm Sci 2018;107:170-82.
49. Censi R, Gigliobianco MR, Dubbini A, Malaj L, Di Martino P. New nanometric solid dispersions of glibenclamide in Neusilin(®) UFL2. AAPS PharmSciTech 2016;17:1204-12.
50. Hentzschel CM, Sakmann A, Leopold CS. Suitability of various excipients as carrier and coating materials for liquisolid compacts. Drug Dev Ind Pharm 2011;37:1200-7.
51. Gupta MK, Vanwert A, Bogner RH. Formation of physically stable amorphous drugs by milling with Neusilin. J Pharm Sci 2003;92:536-51.
52. Jo K, Cho JM, Lee H, Kim EK, Kim HC, Kim H, *et al*. Enhancement of aqueous solubility and dissolution of celecoxib through phosphatidylcholine-based dispersion systems solidified with adsorbent carriers. Pharmaceutics 2018;11:1.
53. Krupa A, Majda D, Jachowicz R, Mozgawa W. Solid-state interaction of ibuprofen and Neusilin US2. Thermochim Acta 2010;509:12-7.
54. Stradi R, Nava D, Nebuloni M, Pastura B, Pini E. Structural elucidation of the rifaximin Ph. Eur. impurity H. J Pharm Biomed Anal 2010;51:858-65.